Passivation Enhancement of Poly-Si Carrier-Selective Contacts by Applying ALD Al_2O_3 Capping Layers

Yang, Guangtao; Van de Loo, Bas; Stodolny, Maciej; Limodio, Gianluca; Melskens, Jimmy; Isabella, Olindo; Weeber, Arthur; Zeman, Miro; Kessels, W. M.M.; More Authors

DOI
10.1109/JPHOTOV.2021.3119595

Publication date
2021

Document Version
Accepted author manuscript

Published in
IEEE Journal of Photovoltaics

Passivation Enhancement of Poly-Si Carrier-Selective Contacts by Applying ALD Al_2O_3 Capping Layers

Guangtao Yang, Bas van de Loo, Maciej Stodolny, Gianluca Limodio, Jimmy Melskens, Bart Macco, Paula Bronsveld, Olindo Isabella, Arthur Weeber, Miro Zeman, and W. M. M. Kessels, *Member, IEEE*

***Abstract*—Hydrogenation of polycrystalline silicon (poly-Si) passivating contacts is crucial for maximizing their passivation performance. This work presents the application of Al_2O_3 prepared by atomic layer deposition as a hydrogenating capping layer. Several important questions related to this application of Al_2O_3 are addressed by comparing results from Al_2O_3 single layers, SiN_x single layers, and Al_2O_3/SiN_x double layers to different poly-Si types. We investigate the effect of the Al_2O_3 thickness, the poly-Si thickness, the poly-Si doping type, and the postdeposition annealing treatment on the passivation quality of poly-Si passivating contacts. Especially, the Al_2O_3/SiN_x stack greatly enhances the passivation quality of both n^+ and p^+ doped as well as intrinsic poly-Si layers. The Al_2O_3 layer thickness is crucial for the single-layer approach, whereas the Al_2O_3/SiN_x stack is less sensitive to the thickness of the Al_2O_3 layer. A thicker Al_2O_3 layer is needed for effectively hydrogenating p^+ compared to n^+ poly-Si passivating contact. The capping layers can hydrogenate poly-Si layers with thicknesses up to at least 600 nm. The hydrogenation-enhanced passivation for n^+ poly-Si is found to be more thermally stable in comparison to p^+ poly-Si. These results provide guidelines on the use of Al_2O_3 capping layers for poly-Si contacts to significantly improve their passivation performance.**

***Index Terms*—Atomic layer deposition (ALD) Al_2O_3, hydrogenation, passivation quality, polycrystalline silicon (poly-Si) passivating contacts, thermal stability.**

I. Introduction

CRYSTALLINE silicon (c-Si) solar cells with polycrystalline silicon (poly-Si) as passivating contacts enable record-high efficiencies due to their excellent passivation and carrier selectivity [1]–[8]. This type of contact consists of an ultrathin SiO_x layer and a heavily doped poly-Si layer on top. So far, most work has focused on improving the quality of poly-Si passivating contacts [9]–[14] and enhancing cell efficiencies. Furthermore, the carrier transport mechanism has been studied as well [15]–[18]. Hydrogenation plays a crucial role in the poly-Si contact formation to achieve outstanding passivation quality [19]–[25]. However, publications that focus specifically on the hydrogenation of poly-Si passivating contacts [8], [10], [19], [25], [28] are fairly limited in comparison to the publications that focus on the development of poly-Si passivating contacts and their application in solar cells [7], [11], [16], [24], [29]–[33]. The passivation of c-Si surfaces by poly-Si relies on two mechanisms: 1) field-effect passivation and 2) chemical passivation [34]. The field-effect passivation is due to the difference in doping level between the heavily doped poly-Si and the lightly doped c-Si bulk, which induces band bending at their interface. This band bending reduces the minority carrier concentration, which, in turn, reduces surface recombination. To maximize this interface band bending, one needs to optimize the doping profile near the poly-Si/SiO_x/c-Si interfaces. On the other hand, an optimum doping profile is necessary but not sufficient in attaining the highest passivation quality. This is because of the thin SiO_x layer (typically $\leq$ 2.2 nm) located between c-Si and poly-Si that is also a crucial factor in the passivation quality. The SiO_x material properties, such as its microstructure as well as its atomic and chemical composition, depend on the preparation method. However, irrespective of the type of SiO_x layer that is used, there always remain some Si bonds at the interface that are not terminated, i.e., Si dangling bonds, and these can act as recombination centers that degrade the chemical passivation [10]. Therefore, an extra step is necessary to passivate these dangling bonds and an effective way to achieve this is by the introduction of hydrogen [7], [35]–[38]. Hydrogenation can be realized with H_2 gas during annealing [34], by a hydrogen-containing remote plasma [39] or by hydrogen-containing capping layers, for example, PECVD SiN_x [4], [28] and atomic layer deposition (ALD) Al_2O_3 and TCO layers followed by thermal annealing [10], [34], [37], [40]–[44]. SiN_x and Al_2O_3 are common materials that are used for surface passivation of c-Si [30], [45], [46]. When annealed at a sufficiently high temperature, the hydrogen in the capping materials can diffuse through the poly-Si materials and passivate the Si-dangling bonds at the SiO_x/c-Si interface. Although they

Manuscript received August 6, 2021; revised October 4, 2021; accepted October 7, 2021. This work was supported by the Topsector Energie of the Dutch Ministry of Economic Affairs under Project AAA TKI TOE1409104. The work of Jimmy Melskens and Bart Macco was supported by The Netherlands Organisation for Scientific Research under the Dutch TTW-VENI under Grant 15896 and Grant 16775, respectively. *(Corresponding authors: Guangtao Yang; W. M. M. Kessels.)*

Guangtao Yang, Gianluca Limodio, Olindo Isabella, and Miro Zeman are with Photovoltaic Materials and Devices Group, Delft University of Technology, 2628 CD Delft, The Netherlands (e-mail: g.yang@tudelft.nl; g.limodio@tudelft.nl; o.isabella@tudelft.nl; m.zeman@tudelft.nl).

Bas van de Loo is with Process Development, SoLayTec, 5651 CA Eindhoven, The Netherlands (e-mail: basvandeloo@gmail.com).

Maciej Stodolny is with New Energies Research and Technology, Shell, 2596 HR The Hague, The Netherlands (e-mail: maciej.stodolny@shell.com).

Jimmy Melskens, Paula Bronsveld, and Arthur Weeber are with TNO Energy Transition, Solar Energy, 1755 LE Petten, The Netherlands (e-mail: jimmy.melskens@tno.nl; paula.bronsveld@tno.nl; a.w.weeber@tudelft.nl).

Bart Macco and W. M. M. Kessels are with the Department of Applied Physics, Eindhoven University of Technology, 5612 AZ Eindhoven, The Netherlands (e-mail: b.macco@tue.nl; w.m.m.kessels@tue.nl).

Color versions of one or more figures in this article are available at https://doi.org/10.1109/JPHOTOV.2021.3119595.

Digital Object Identifier 10.1109/JPHOTOV.2021.3119595

have proven to be effective capping layers for hydrogenation, more practical insights into the application of the Al_2O_3-based capping layers on hydrogenating of poly-Si carrier selective contacts should be obtained, which is the focus of this work.

To decouple the influence of the field-effect passivation due to the heavy doping of the poly-Si layers from the influence of the chemical passivation owing to the hydrogen passivation, different types of poly-Si (intrinsic, n^+, and p^+ type) were studied in this work. Furthermore, the dependence of the poly-Si passivation enhancement induced by several parameters used during the hydrogenation process has not been clarified thus far. Therefore, we have studied different capping layers (including ALD Al_2O_3, PECVD SiN_x, and Al_2O_3/SiN_x double-layer capping) with a focus on the influence of the Al_2O_3 thickness, the PECVD SiN_x layer, the poly-Si layer doping types and thicknesses, and the annealing temperature. Finally, the thermal stability of the enhanced poly-Si passivation enabled by different types of hydrogenation approaches was analyzed.

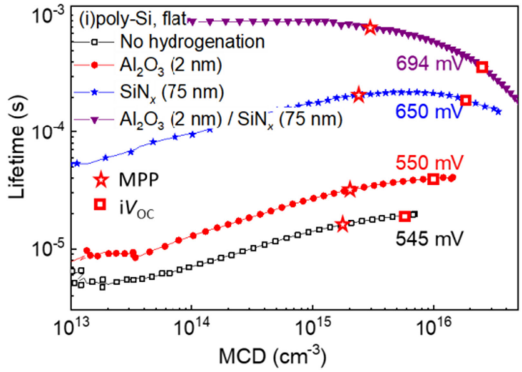

Fig. 1. Effective lifetime as a function of minority carrier density (MCD, the injection level) of the symmetrical test samples before hydrogenation and after hydrogenation for 150-nm thick intrinsic poly-Si. For all the samples with the capping layer(s), an FGA step at 400 °C is carried out before the lifetime measurement. The MCD at MPP [46] and the point and value of the one-sun implied open-circuit voltage (iV_{OC}) are calculated and indicated for the curves.

II. Experiment

Double-side polished n-FZ wafers with a resistivity of 1-5 $\Omega\cdot$cm and $<100>$ orientation were used in this work. The thickness of the wafers before texturing with TMAH (trimethylammonium hydroxide) was 280 ± 20 μm. On all symmetrical passivation test samples, a thin SiO_x layer was grown by nitric acid oxidation of silicon (NAOS) [45] or thermal oxidation (th-SiO_x) [31]. Subsequently, intrinsic LPCVD poly-Si ((i)poly-Si) layers were deposited on both sides. The deposition time was adjusted for poly-Si deposition on textured c-Si surfaces to obtain a poly-Si layer with an effective thickness of 150 nm, which is the same as that on flat c-Si surfaces. Doping was introduced via phosphorous ion implantation on both sides of the samples with the energy of 20 keV and dose of 6×10^{15} cm^{-2} for n^+ poly-Si [45] or via BBr_3 diffusion for p^+ poly-Si [31]. For the n^+ poly-Si, a subsequent high-temperature annealing treatment at 950 °C for 5 min was applied to activate and diffuse the dopants. To study the dependence of the hydrogenation on the poly-Si layer thickness, poly-Si samples with different thicknesses were prepared. For these n^+ poly-Si samples with different thicknesses, the same high-temperature annealing process was used to activate the ion-implanted phosphorous. Due to the differences in the poly-Si layer thickness, different phosphorous doping profiles at the c-Si/SiO_x/poly-Si interfaces can be expected for these samples as was shown in our previous study [32], which should, in turn, induce differences in the levels of field-effect passivation. All the samples used in this work were one-quarter of 4-in. round wafers, which were cut before the deposition of the capping layer(s).

Three hydrogenation approaches were compared in this work:

1) ALD Al_2O_3 capping layers with different thicknesses;
2) PECVD SiN_x capping layers;
3) Al_2O_3/SiN_x double capping layers.

An HF dip was conducted before the deposition of the capping layers. The Al_2O_3 layers were deposited by thermal ALD in an Oxford Instruments OpAL reactor at a substrate temperature of 200 °C. Trimethylaluminum [$Al(CH_3)_3$] and H_2O were used as the metal precursor and coreactant, respectively. The ALD cycle time was ~7 s and the growth per cycle was 1.1 Å [46]. The ALD cycles were repeated until the target film thicknesses (from 2 to 16 nm) were reached. The SiN_x layers were deposited in an Oxford Instruments PECVD reactor at a substrate temperature of 400 °C with SiH_4 and NH_3 as precursors. The deposition rate was 15 nm/min for flat surfaces. To obtain similar SiN_x layer thicknesses for flat and pyramid textured Si surfaces, the deposition time for textured samples was multiplied by 1.73 to account for the difference in an effective area between the pyramid textured facets and flat surfaces. After deposition of the capping layers, all samples received an annealing treatment at 400 °C for 30 min in forming gas (10% H_2 in N_2 atmosphere, also known as forming gas annealing, FGA) before measuring the passivation quality. Different FGA temperatures and times were used to test the thermal stability of the passivation quality achieved by the aforementioned hydrogenation approaches. The lifetime and implied open-circuit voltage (iV_{OC}) of the samples were analyzed in a Sinton WCT-120 lifetime tester applying the generalized measurement mode [47].

III. Results

We first studied the influence of the poly-Si doping type on the enhancement of the passivation quality for poly-Si samples with different hydrogenating capping layers. For (i)poly-Si, the initial passivation levels are very low, with an iV_{OC} of 545 mV before any hydrogenation process, see Fig. 1. By capping the sample with 2-nm-thick Al_2O_3 and conducting a subsequent FGA, the passivation quality is slightly enhanced. The enhancement of the passivation quality that is induced by a 75-nm-thick SiN_x layer followed by an FGA treatment is much larger, resulting in a clear increase in minority carrier lifetime and an iV_{OC} of 650 mV. However, when combining both materials in the form of a 2-nm-thick Al_2O_3 layer covered with a 75-nm-thick SiN_x capping layer, we observe the largest enhancement of the passivation quality for (i)poly-Si. The minority carrier lifetime of this sample almost reaches 1 ms with an iV_{OC} of 694 mV. When

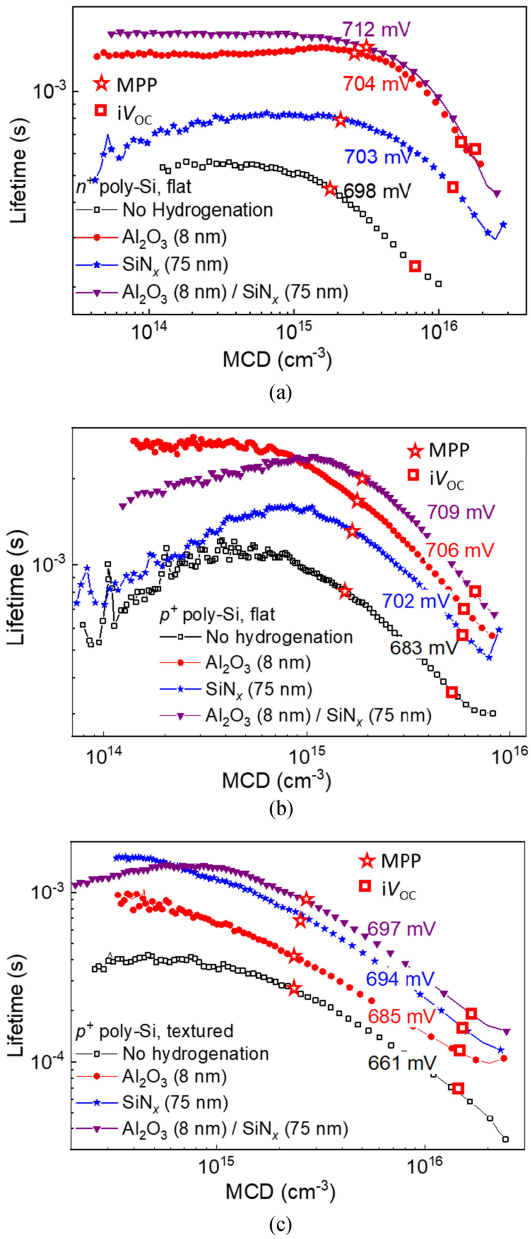

Fig. 2. Effective lifetime as a function of minority carrier density (MCD, the injection level) of the symmetrical test samples before hydrogenation and after hydrogenation for 150-nm thick (a) n^+ doped and (b) p^+ doped poly-Si prepared on flat c-Si surfaces with NAOS as interfacial SiO_x, and (c) 150-nm p^+ doped poly-Si prepared on a textured c-Si surface with th-SiO_x as interfacial SiO_x. For all the samples with the capping layer(s), an FGA step at 400 °C is carried out before the lifetime measurement. The doping levels for B and P are higher than 1×10^{20} cm^{-3}; the doping profiles of the n^+ and p^+ doped poly-Si samples are given in [33] and [64]. The MCD at MPP [48] and the point and value of the one-sun implied open-circuit voltage (iV_{OC}) are calculated and indicated for the curves.

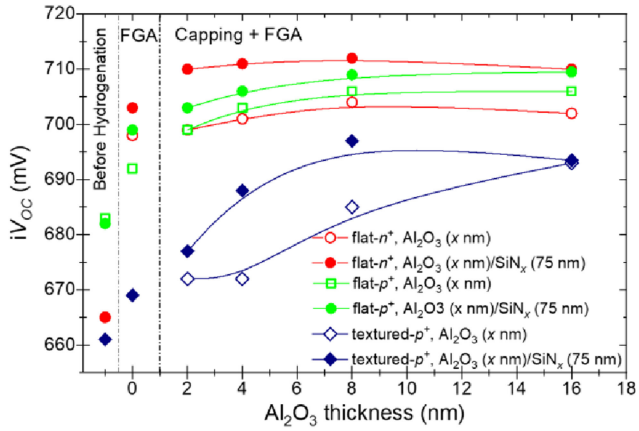

Fig. 3. Passivation performance (iV_{OC}) of both 150-nm thick n^+ and p^+(on planar wafers) and p^+ (on textured wafers) poly-Si layers after hydrogenation with Al_2O_3 and Al_2O_3/SiN_x capping layer approaches, as a function of the Al_2O_3 layer thickness (denoted as "x"). The cases for 0-nm Al_2O_3 stands for samples without a capping layer but only experienced FGA treatment. All the FGA steps were conducted at 400 °C for 30 min. The lines serve as a guide to the eyes.

comparing the same hydrogenation approaches for n^+ and p^+ doped poly-Si samples, we also find that the Al_2O_3 /SiN_x double capping layer performs the best, as shown in Fig. 2(a) and (b). Due to the presence of field-effect passivation introduced by the heavy doping within the poly-Si, as well as a possible gettering effect by the dopants, the lifetime measured for both doped samples before hydrogenation is much higher in comparison to the (i)poly-Si sample. For n^+ and p^+ doped poly-Si on planar surfaces, we find that the enhancement in passivation quality by applying a 75-nm-thick SiN_x followed by FGA treatment is small compared to the approaches of a single Al_2O_3 (8 nm) capping layer or an Al_2O_3 (8 nm)/SiN_x (75 nm) double capping layer. In order to see whether the abovementioned trends, obtained on a flat c-Si surface with NAOS-SiO_x as interlayer, are invariant of the type of c-Si surface morphology and the preparation method of SiO_x interlayer, the three different hydrogenation approaches were also tested for a more challenging case, i.e., p^+ poly-Si on textured Si surfaces with thermal-SiO_x as interlayer, see Fig. 2(c). We find that a 75-nm-thick SiN_x layer with a subsequent FGA can hydrogenate the p^+ poly-Si samples well, but also in this case, with an extra 8-nm-thick Al_2O_3 layer between the p^+ poly-Si and the SiN_x layer the passivation quality is enhanced the most when looking at the high injection level around maximum power point (MPP) [48].

In order to study the dependence of the passivation quality enhancement on the Al_2O_3 layer thickness, we choose samples with three cases: n^+ and p^+ doped poly-Si on a flat surface that gives the high passivation quality and p^+ doped poly-Si on a textured surface, which gives the lowest passivation quality. The results are shown in Fig. 3. We found that an FGA treatment does not yield very high iV_{OC} values and, therefore, is not providing adequate passivation. The capping by Al_2O_3 or Al_2O_3/SiN_x followed by annealing enhances the passivation performance significantly. In both these hydrogenation approaches, increasing the Al_2O_3 layer thickness generally enhances the passivation quality up to a thickness of around 8 nm. A further increase in the Al_2O_3 layer thickness does not help in enhancing the passivation quality, except for textured p^+ poly-Si samples with an Al_2O_3 single capping layer. Considering that the Al_2O_3 thicknesses are the same on the flat p^+ poly-Si surface and the textured p^+ poly-Si facets due to the excellent conformality of the ALD technique, we conclude that textured p^+ poly-Si

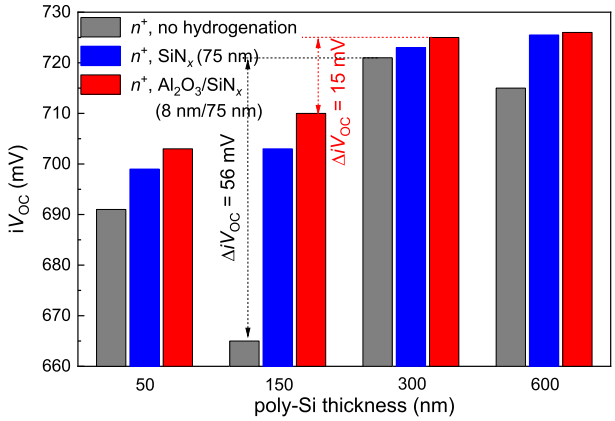

Fig. 4. Passivation enhancement by hydrogenation for n$^+$ poly-Si with different thicknesses. All the poly-Si samples were prepared with the same process, which is optimized for 300-nm thick poly-Si. For all the samples with the capping layer(s), an FGA step at 400 °C was carried out before the lifetime measurement. The ΔiV_{OC} values between the optimized (300 nm) and one of the nonoptimized (150 nm) samples are indicated in the figure.

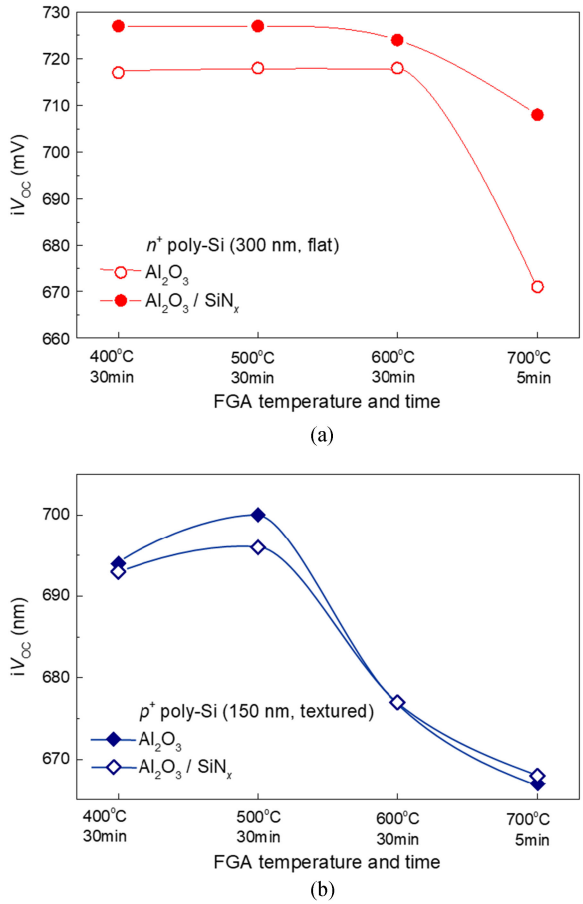

Fig. 5. Thermal stability test of passivation for hydrogenated (a) 300-nm-thick flat n+ and (b) 150-nm-thick textured p+ poly-Si on a textured Si surface. The FGA is executed directly after capping. The Al_2O_3 layer is 8-nm thick. The lines serve as a guide to the eyes.

samples need a thicker Al_2O_3 layer for a further enhancement of the passivation quality. Furthermore, the fact that the dependence of the enhancement in passivation quality on the Al_2O_3 layer thickness is more pronounced for p^+ on the textured surface than it is for p^+ and n^+ poly-Si samples on flat surfaces can also be related to the difference between planar and textured surfaces. Comparing the two hydrogenation approaches shown in Fig. 3, for both n^+ and p^+ poly-Si samples, the Al_2O_3/SiN_x approach presents a larger enhancement in comparison to the single Al_2O_3 capping layer approach.

In order to study the dependence of the hydrogenation-induced passivation enhancement on the poly-Si layer thickness, we intentionally prepared samples with a large variation in the poly-Si layer thicknesses. First, we selected a type of n^+ poly-Si, which was optimized for a 300-nm-thick poly-Si sample in terms of doping profile for achieving the highest field-effect passivation before hydrogenation. Next, we used the same process parameters, i.e., the same NAOS-SiO_x, P-implantation, and high-temperature annealing to prepare samples with different poly-Si thicknesses (50, 150, and 600 nm). As a consequence, these samples are not prepared at their optimum conditions, in terms of implantation and annealing parameters. Especially for the thin poly-Si samples, when using the same implantation and annealing parameters as that for the optimized 300-nm-thick poly-Si sample, a much deeper and higher doping level of P in-diffusion to the c-Si bulk is expected, which was already observed in our previous work [32]. Therefore, lower passivation qualities are obtained for these samples than that for the optimized 300-nm-thick poly-Si one, see Fig. 4. Since the SiN_x layer is commonly used in TOPCon solar cells, for example, the i-TOPCon [65], as hydrogenation and antireflection layer, we presented the passivation results of poly-Si samples prepared with 75-nm-thick SiN_x and Al_2O_3(8 nm)/SiN_x(75 nm) hydrogenation approaches, which can be seen in Fig. 4. Again, the Al_2O_3/SiN_x double capping layer approach gives a larger enhancement in passivation than the SiN_x single capping layer approach. Moreover, for the optimized 300-nm-thick flat n^+ poly-Si, the enhancement due to the hydrogenation is less clear, when compared to the nonoptimized samples. Especially for the 150-nm-thick poly-Si sample, the enhancement is very pronounced, which brings its passivation quality back to the trend of their dependence on the poly-Si thickness.

In the previous work, the hydrogenation-induced passivation quality proved to be thermally stable against a metal paste firing process [30]. However, the exposure of the poly-Si samples at the firing peak temperature is only a few seconds. To find the threshold thermal budget that degrades the hydrogenation effect and to compare the hydrogenation approaches in this respect, we also tested the thermal stability of the passivation quality after hydrogenation with Al_2O_3 or Al_2O_3/SiN_x capping approaches. The accumulative annealing treatments used for these tests were conducted in forming gas with different thermal budgets. As shown in Fig. 5(a), the passivation quality in the case of flat n^+ poly-Si can withstand a 30-min-long FGA treatment at 600 °C. However, when increasing the annealing temperature to 700 °C, even after only 5 min of FGA, the n^+ poly-Si loses its passivation quality. This is especially the case for the single Al_2O_3 capping layer approach, whereas the sample with a double capping

layer still shows good passivation quality with iV_{OC} exceeding 710 mV. In this respect, the Al_2O_3/SiN_x double-layer capping appears to be more thermally stable than the single Al_2O_3 capping layer, in addition to also enabling a higher passivation quality. For p^+ poly-Si on a textured surface, see Fig. 5(b), the high passivation quality is maintained after a 30-min-long FGA treatment at 500 °C. However, when using a higher annealing temperature, e.g., 30-min-long FGA at 600 °C or 5-min-long FGA at 700 °C, a deterioration of the passivation quality is observed for both the single Al_2O_3 and Al_2O_3/SiN_x double-layer capping approaches. The obtained iV_{OC} values are below 680 mV, similar to the values reported before hydrogenation in Fig. 3.

IV. Discussion

The field-effect passivation established on the c-Si surface using (i)poly-Si is very weak and the overall passivation is largely governed by chemical passivation provided by the tunnel SiO_x layer. By passivating the Si-dangling bonds at the poly-Si/SiO_x/c-Si interface with hydrogen, an enhanced level of chemical passivation is found, as shown in Fig. 1. For the (i)poly-Si samples, we compared the hydrogenation effects of the abovementioned three different approaches. The minor enhancement of iV_{OC} to 550 mV for the approach of Al_2O_3 capping followed by FGA is mainly due to the limited chemical passivation enhancement by the ultrathin Al_2O_3 capping layer which is only 2-nm thick [46], [49], [50]. When increasing the Al_2O_3 thickness to 32 nm, the iV_{OC} increased to 687 mV (the lifetime curve is not shown here). It is plausible that, when a thicker Al_2O_3 layer is applied, more hydrogen is available to be released upon annealing when compared to a thinner Al_2O_3 layer. Upon annealing, the released hydrogen can diffuse to the c-Si interface and passivate the Si dangling bonds or effuse out without contributing to passivation [51]. Therefore, it can be expected that the probability that dangling bonds at the c-Si interface become bonded with hydrogen increases with increasing the Al_2O_3 layer thickness. At a certain FGA condition, by increasing the Al_2O_3 capping thickness beyond a certain value, the amount of hydrogen atoms that can be bonded at the interfaces saturates. At that point, the amount of hydrogen in the capping layer will not be a limiting factor for the passivation enhancement. The passivation quality enhancement depending on the thickness of Al_2O_3 single capping layer is tested for n^+ and p^+ poly-Si samples, as shown in Fig. 3. For n^+ poly-Si samples, the enhancement of the passivation saturates when increasing the Al_2O_3 single capping layer to 8 nm while a thicker Al_2O_3 single capping layer is needed to obtain optimized passivation for the (textured) p^+ poly-Si sample.

Based on the discussion above on the influence of the Al_2O_3 thickness on the hydrogenation effect and the results shown in Fig. 3, we speculate that a key point for hydrogenation is to balance the diffusion of the hydrogen contained in the capping layer to the c-Si/SiO_x/poly-Si interfaces and the effusion of the hydrogen into the ambient [42], [51]. Therefore, to enhance the hydrogenation effect, the thin Al_2O_3 layer can also be capped with a material that can act as a good hydrogen effusion barrier, and/or has a higher hydrogen content. The latter would reverse the gradient in the hydrogen concentration when going toward the ambient. Among the commonly used materials for this purpose, PECVD SiN_x is one of the most straightforward choices, which is normally used as a passivation layer and antireflection coating (ARC) on solar cells [4], [52]–[55]. PECVD SiN_x has an atomic hydrogen concentration at around 10%–15% [56], which is higher than the 2–4 at. % in an Al_2O_3 layer deposited at 200 °C. Although the temperature dependence of the hydrogen diffusion rates for Al_2O_3 and SiN_x materials are different, the hydrogen diffusion coefficient within these two materials appears to be similar, on the order of 10^{-19} cm^2/s, at the studied, moderate temperatures (∼400 °C) [56], [57]. If the hydrogenation would only depend on the amount of hydrogen in the capping layer(s), replacing the thin Al_2O_3 capping layer with a much thicker (75-nm thick) SiN_x layer would lead to a further improvement in passivation. However, this is not the case. The passivation enhancement on flat c-Si surfaces for n^+ poly-Si samples [shown in Fig. 2(a)] and p^+ poly-Si samples [shown in Fig. 2(b)] due to the hydrogenation with 75-nm-thick SiN_x is not as high as that provided by 8-nm-thick Al_2O_3. This means that when the Al_2O_3 thickness exceeds the aforementioned saturation threshold, the amount of hydrogen in the capping layer(s) is not the dominating factor for hydrogenating n^+ and p^+ poly-Si on flat surfaces. The way that hydrogen is bonded in the Al_2O_3 and released from the film seems also to play a very important role for the effective passivation induced by the Al_2O_3 as has also been discussed for passivation of c-Si before [50], [58]. For the case of textured Si surfaces, the passivation quality provided by p^+ poly-Si benefits more from a 75-nm-thick SiN_x single capping layer than from an 8-nm-thick Al_2O_3 single capping layer, as shown in Fig. 2(c). This could possibly be related to the differences between <111>-oriented surfaces and <100>-oriented surfaces [59] as well as to a larger surface area for the textured surface (also due to the presence of nanotextures on the pyramid facets). For the textured surface, we speculate that the amount of hydrogen diffused from the 8-nm-thick Al_2O_3 layer into the c-Si surface with the applied annealing processes is not enough to reach the "saturation threshold." In order to enhance the passivation, a higher amount of hydrogen is required to increase the probability of forming Si-H bonds to terminate the Si dangling bonds. The larger content of hydrogen within the 75-nm-thick SiN_x layer compared to the 8-nm-thick Al_2O_3 layer could be helpful in this respect. This would be consistent with the results shown in Fig. 3, in the sense that the amount of hydrogen within the 16-nm-thick Al_2O_3 single capping layer that diffuses to the c-Si/SiO_x/poly-Si interface is still not enough to fully hydrogenate the sample with p^+ poly-Si on a textured Si surface. This implies that in the case of textured p^+ poly-Si samples more hydrogen is needed to hydrogenate the interfaces compared to what is needed for flat samples.

It is found that by applying an FGA treatment at 400 °C for 30 min, the Al_2O_3 single capping layer approach for hydrogenating flat poly-Si samples is better than the SiN_x single capping layer. As a consequence, a higher passivation enhancement can be expected for the Al_2O_3/SiN_x double capping layer approach, which combines the better hydrogenation capability from the

Al_2O_3 capping layer with the higher hydrogen content properties from SiN_x layers. This is an approach that is similar to what is used for c-Si surface passivation, by the Al_2O_3/SiN_x double-layer [60]. It is found that for all cases considered here, irrespective of the poly-Si doping type or the c-Si surface morphology (see Figs. 1–3), the Al_2O_3/SiN_x double capping layer hydrogenation approach yields the highest passivation quality. For flat n^+ poly-Si samples, the SiN_x capping makes it possible to reduce the Al_2O_3 layer thickness from 8 to 2 nm while still obtaining the highest passivation enhancement compared to the Al_2O_3 single capping layer approach. For samples with p^+ poly-Si on textured Si surfaces with the SiN_x capping, an 8-nm-thick Al_2O_3 layer is enough to achieve the highest passivation enhancement. This means that when applying a SiN_x layer on top of Al_2O_3, the dependence of the hydrogenation effect on the Al_2O_3 thickness becomes less pronounced. However, the presence of Al_2O_3 is crucial for obtaining the best level of hydrogenation, as can be concluded from a comparison of the SiN_x single capping approach to the Al_2O_3/SiN_x double capping layer approach. It is especially true for the (i)poly-Si samples, even though the Al_2O_3 is as thin as 2 nm. As mentioned, it is not just related to the amount of hydrogen present in the stack, the way that hydrogen is bonded in the Al_2O_3 and released from the film during annealing seems to play a very important role too. The fact that a thin SiO_x layer (< 2 nm) develops at the poly-Si/Al_2O_3 interface during the deposition and annealing processes and that there is a difference in fixed charges for the Al_2O_3/SiN_x and SiN_x cases is not expected to play a significant role. The surface recombination mainly happens at the c-Si/SiO_x/(i)poly-Si interface and the depletion region induced by the fixed charges within the capping layer is expected not to extend to the c-Si surface for the 150-nm-thick (i)poly-Si.

As shown in Figs. 1 and 2, the passivation quality of poly-Si samples of all the doping types can be enhanced by the applied hydrogenation approaches. As discussed earlier, the Al_2O_3/SiN_x stack is a highly effective hydrogenation approach for both intrinsic and doped (n^+ and p^+) poly-Si samples. Compared to the (i)poly-Si samples, the doped poly-Si samples show much higher passivation qualities due to the presence of the field-effect passivation and potentially due to the differences in the type and density of defects in the ultra-thin SiO_x layer, which becomes doped with P (SiO_x:P) or B (SiO_x:B) after diffusion. The latter is, however, expected to be the same for samples with the same doping type, independent of the deposition of hydrogenating capping layer(s) leading to hydrogenation. On the other hand, due to the presence of the field-effect passivation in the doped poly-Si samples, the absolute gain in iV_{OC} values due to hydrogenation is not as high as it is for the (i)poly-Si samples.

An additional strong benefit of hydrogenation is that it can minimize variations in passivation levels due to nonoptimal doping processes or variations in a poly-Si layer thickness. Because the same process steps were used for all the samples shown in Fig. 4, when varying the poly-Si layer thickness, the doping profile (for thinner poly-Si samples) and doping level (for thicker poly-Si samples) will not be as optimal as that in the optimized 300-nm-thick poly-Si sample. If we assume that the ultra-thin SiO_x:P interlayers are all similar for all the n^+ poly-Si samples, the doping profile and level differences lead to the field-effect passivation quality differences between samples, therefore, their overall passivation qualities. Therefore, the field-effect passivation qualities of these nonoptimized samples are not as high as the optimized case, the 300-nm poly-Si sample, which can be seen from the differences in iV_{OC} values of these samples before hydrogenation, shown in Fig. 4. However, after hydrogenation, the enhancement in overall passivation quality of the optimized 300-nm-thick n^+ poly-Si sample is less pronounced when compared to the nonoptimized samples, especially for the 150-nm-thick poly-Si sample. Interestingly, after hydrogenation, the ΔiV_{OC} values from wafer to wafer due to the poly-Si thickness variation, between 50 and 600 nm, are suppressed. This indicates that an effective hydrogenation process, which maximizes the chemical passivation, can partly compensate for a relatively poor field-effect passivation and induce a high overall passivation quality.

Due to the fact that a 75-nm-thick SiN_x layer acts as a hydrogen effusion barrier for the Al_2O_3 layer, capping the Al_2O_3 layer with SiN_x should be more thermally stable against the hydrogen loss during a high-temperature treatment. This is indeed observed for n^+ poly-Si samples, as is shown in Fig. 5(a): A smaller drop in passivation quality is observed for the sample capped with an Al_2O_3/SiN_x double capping layer when compared to the sample with a single Al_2O_3 capping layer after annealing at 700 °C for 5 min. However, for the 150-nm-thick p^+ poly-Si on a textured Si surface, a similar trend is observed for both hydrogenation approaches [see Fig. 5(b)] and the drop in passivation quality is observed at a lower temperature in comparison to the n^+ poly-Si sample. Despite the difference in poly-Si thickness, we believe this is not the dominant factor for dehydrogenation/effusion of hydrogen for these poly-Si samples, since these poly-Si layer thickness values are higher than that for the capping layers. Also since our samples are capped, the H effusion is likely limited by the capping layer rather than the poly-Si layer thickness. Therefore, we conclude that n^+ poly-Si is more thermally stable than p^+ poly-Si. This may be due to the fact that hydrogen incorporation is less thermally stable in p^+ poly-Si compared to n^+ poly-Si. Something similarly has been reported for a-Si:H(p) and a-Si:H(n) in silicon heterojunction (SHJ) interfaces [61]. In the SHJ structure, hydrogen effusion is more energetically favorable for p-type a-Si:H, when E_F is close to the valence band, which induces lower thermal stability in comparison to n-type a-Si:H. For the hydrogenated p^+ poly-Si samples, it still needs to be clarified whether the observed lower thermal stability for p^+ poly-Si samples compared to n^+ poly-Si samples can be attributed to similar reasons [26], [27], [42], [62], [63]. Obviously, the overall passivation quality provided by the Al_2O_3/SiN_x double capping layer approach is not significantly better than the Al_2O_3 single-layer approach for p^+ poly-Si. With a better understanding of the thermal stability of the hydrogenation-enhanced passivation, the superior performance of the double-layer approach may become apparent also in the case of p^+ poly-Si.

V. Conclusion

In this work, the application of ALD Al_2O_3 as a hydrogenating capping layer for poly-Si is extensively studied. Hydrogenation approaches for poly-Si capped by ALD Al_2O_3, PECVD SiN_x, and ALD Al_2O_3 combined with PECVD SiN_x are compared. Application of any of these capping layers to n^+, p^+, and (i)poly-Si will result in an enhancement of the passivation quality. The final passivation quality strongly depends on the ALD Al_2O_3 thickness in the case of a single capping layer approach, whereas this is much less pronounced for the Al_2O_3/SiN_x stack, especially in the case of n^+ poly-Si samples. The Al_2O_3/SiN_x stack was demonstrated to be the most effective approach for hydrogenating poly-Si among all of the tested hydrogenation approaches. Nonoptimal field-effect passivation quality due to the doping or variations in poly-Si thickness can be compensated by effective hydrogenation, which induces a high level of chemical passivation. Additionally, capping the Al_2O_3 layer with SiN_x, which acts as a hydrogen effusion barrier, improves the thermal stability of the hydrogenated n^+ poly-Si samples. These findings show a promise for the application of the Al_2O_3/SiN_x stack for the effective hydrogenation of poly-Si-based passivating contacts.

References

[1] E. Yablonovitch, T. Gmitter, R. M. Swanson, and Y. H. Kwark, "A 720 mV open circuit voltage SiO_x:C-Si:SiO_x double heterostructure solar cell," *Appl. Phys. Lett.*, vol. 47, 1985, Art. no. 1211.

[2] S. W. Glunz *et al.*, "The irresistible charm of a simple current flow pattern – 25% with a solar cell featuring a full-area back contact," in *Proc. 31st Eur. Photovolt. Sol. Energy Conf. Exhib.*, 2015, pp. 259–263.

[3] U. Römer *et al.*, "Ion implantation for poly-Si passivated back-junction back-contacted solar cells," *IEEE J. Photovolt.*, vol. 5, no. 2, pp. 507–514, Mar. 2015.

[4] D. Yan, A. Cuevas, J. Bullock, Y. Wan, and C. Samundsett, "Phosphorus-diffused polysilicon contacts for solar cells," *Sol. Energy Mater. Sol. Cells*, vol. 142, pp. 75–82, 2015.

[5] Y. Chen *et al.*, "Mass production of industrial tunnel oxide passivated contacts (i-TOPCon) silicon solar cells with average efficiency over 23% and modules over 345 W," *Prog. Photovolt. Res. Appl.*, vol. 27, no. 10, pp. 827–834, 2019.

[6] S. W. Reichel *et al.*, "Interdigitated back contact silicon solar cells featuring ion-implanted poly-Si/SiO_x passivating contacts," in *Proc. 33th Eur. Photovolt. Sol. Energy Conf. Exhib.*, 2017, pp. 455–459.

[7] F. Haase *et al.*, "Laser contact openings for local poly-Si-metal contacts enabling 26.1%-efficient POLO-IBC solar cells," *Sol. Energy Mater. Sol. Cells*, vol. 186, pp. 184–193, Nov. 2018.

[8] J. Polzin *et al.*, "Thermal activation of hydrogen for defect passivation in poly-Si based passivating contacts," *Sol. Energy Mater. Sol. Cells*, vol. 230, 2021, Art. no. 111267.

[9] J. Steffens, J. Rinder, G. Hahn, and B. Terheiden, "Compensation of the sputter damage during a-Si deposition for poly-Si/SiO_x passivating contacts by ex-situ P-doping," *AIP Conf. Proc.*, vol. 2147, pp. 040018-1–040018-5, Aug. 2019.

[10] B. Nemeth *et al.*, "Polycrystalline silicon passivated tunneling contacts for high efficiency silicon solar cells," *J. Mater. Res.*, vol. 31, no. 6, pp. 671–681, 2016.

[11] F. Feldmann *et al.*, "High and low work function materials for passivated contacts," *Energy Procedia*, vol. 77, pp. 263–270, 2015.

[12] M. Hayes *et al.*, "Impurity gettering by boron- and phosphorus-doped polysilicon passivating contacts for high-efficiency multicrystalline silicon solar cells," *Phys. Status Solidi Appl. Mater. Sci.*, vol. 216, no. 17, pp. 1–8, 2019.

[13] A. Richter *et al.*, "Tunnel oxide passivating electron contacts as full-area rear emitter of high-efficiency p-type silicon solar cells," *Prog. Photovolt. Res. Appl.*, vol. 26, no. 8, pp. 579–586, 2018.

[14] G. Nogay *et al.*, "Interplay of annealing temperature and doping in hole selective rear contacts based on silicon-rich silicon-carbide thin films," *Sol. Energy Mater. Sol. Cells*, vol. 173, pp. 18–24, Dec. 2017.

[15] F. Feldmann *et al.*, "Tunnel oxide passivated contacts as an alternative to partial rear contacts," *Sol. Energy Mater. Sol. Cells*, vol. 131, pp. 46–50, 2014.

[16] D. Yan, A. Cuevas, Y. Wan, and J. Bullock, "Passivating contacts for silicon solar cells based on boron-diffused recrystallized amorphous silicon and thin dielectric interlayers," *Sol. Energy Mater. Sol. Cells*, vol. 152, pp. 73–79, 2016.

[17] T. F. Wietler *et al.*, "Pinhole density and contact resistivity of carrier selective junctions with polycrystalline silicon on oxide," *Appl. Phys. Lett.*, vol. 110, no. 25, pp. 253902-1–253902-5, 2017.

[18] N. Folchert *et al.*, "Temperature-dependent contact resistance of carrier selective poly-Si on oxide junctions," *Sol. Energy Mater. Sol. Cells*, vol. 185, pp. 425–430, Oct. 2018.

[19] B. W. H. van de Loo *et al.*, "On the hydrogenation of poly-Si passivating contacts by Al_2O_3 and SiN_x thin films," *Sol. Energy Mater. Sol. Cells*, vol. 215, 2020, Art. no. 110592.

[20] T. N. Truong *et al.*, "Deposition pressure dependent structural and optoelectronic properties of ex-situ boron-doped poly-Si/SiO_x passivating contacts based on sputtered silicon," *Sol. Energy Mater. Sol. Cells*, vol. 215, Apr. 2020, Art. no. 110602. [Online]. Available: https://doi.org/10.1016/j.solmat.2020.110602

[21] F. Feldmann *et al.*, "Large area TOPCon cells realized by a PECVD tube process," in *Proc. 36th Eur. Photovolt. Sol. Energy Conf. Exhib.*, 2019, pp. 304–308.

[22] C. Hollemann *et al.*, "Separating the two polarities of the POLO contacts of an 26.1%-efficient IBC solar cell," *Sci. Rep.*, vol. 10, no. 1, pp. 1–15, 2020.

[23] Z. Zhang *et al.*, "Improvement of passivation quality by post-crystallization treatments with different methods for high quality tunnel oxide passivated contact c-Si solar cells," in *Proc. IEEE 46th Photovolt. Spec. Conf.*, 2020, pp. 2215–2218.

[24] A. Ingenito *et al.*, "Phosphorous-doped silicon carbide as front-side full-area passivating contact for double-side contacted c-Si solar cells," *IEEE J. Photovolt.*, vol. 9, no. 2, pp. 346–354, Mar. 2019.

[25] G. Kaur *et al.*, "Ultra-thin LPCVD SiN_x/n^+-poly-Si passivated contacts—A possibility?," in *Proc. Conf. Rec. IEEE Photovolt. Spec. Conf*, 2019, pp. 2679–2683.

[26] M. Schnabel *et al.*, "Hydrogen passivation of poly-Si/SiO_x contacts for Si solar cells using Al_2O_3 studied with deuterium," *Appl. Phys. Lett.*, vol. 112, no. 20, 2018, Art. no. 203901.

[27] B. W. H. van de Loo *et al.*, "On the hydrogenation of poly-Si passivating contacts by Al_2O_3 and SiN_x thin films," *Sol. Energy Mater. Sol. Cells*, vol. 215, 2020, Art. no. 110592.

[28] B. Hoex, J. Schmidt, P. Pohl, M. C. M. van de Sanden, and W. M. M. Kessels, "Silicon surface passivation by atomic layer deposited Al_2O_3," *J. Appl. Phys.,* vol. 104, no. 4, pp. 044903-1–044903-12, 2008. [Online]. Available: https://doi.org/10.1063/1.2963707

[29] U. Römer *et al.*, "Ion-implanted poly-Si/c-Si junctions as a back-surface field in back-junction back-contacted solar cells," in *Proc. 29th Eur. Photovolt. Sol. Energy Conf.*, 2014, pp. 1107–1110.

[30] M. K. Stodolny *et al.*, "Material properties of LPCVD processed n-type polysilicon passivating contacts and its application in PERPoly industrial bifacial solar cells," *Energy Procedia*, vol. 124, pp. 635–642, Sep. 2017.

[31] I. G. R. M. K. Stodolny *et al.*, "Novel schemes of p^+ poly-Si hydrogenation implemented in industrial 6" bifacial front-and-rear passivating contacts solar cells," in *Proc. 35th Eur. Photovolt. Sol. Energy Conf. Exhib.*, 2018, pp. 414–417.

[32] G. Limodio *et al.*, "Implantation-based passivating contacts for crystalline silicon front/rear contacted solar cells," *Prog. Photovolt. Res. Appl.*, vol. 28, pp. 403–416, 2020.

[33] Y. Yang, "Recent progress at Trina in large area IBC cells with passivated contacts," in *Proc. 8th Int. Conf. Cryst. Silicon Photovolt.*, 2018.

[34] J. Melskens *et al.*, "Passivating contacts for crystalline silicon solar cells: From concepts and materials to prospects," *IEEE J. Photovolt.*, vol. 8, no. 2, pp. 373–388, Mar. 2018.

[35] L. E. Black *et al.*, "Explorative studies of novel silicon surface passivation materials: Considerations and lessons learned," *Sol. Energy Mater. Sol. Cells*, vol. 188, pp. 182–189, 2018.

[36] J. Temmler *et al.*, "Inline PECVD deposition of poly-Si-based tunnel oxide passivating contacts," *Phys. Status Solidi Appl. Mater. Sci.*, vol. 215, no. 23, pp. 1–4, 2018.

[37] T. N. Truong *et al.*, "Hydrogenation of phosphorus-doped polycrystalline silicon films for passivating contact solar cells," *ACS Appl. Mater. Interfaces*, vol. 11, no. 5, pp. 5554–5560, 2019.

[38] Y. Wan, K. R. McIntosh, and A. F. Thomson, "Characterisation and optimisation of PECVD sinx as an antireflection coating and passivation layer for silicon solar cells," *AIP Adv.,* vol. 3, no. 3, pp. 032113-1–032113-14, 2013.

[39] P. Repo, H. Talvitie, S. Li, J. Skarp, and H. Savin, "Silicon surface passivation by Al_2O_3: Effect of ALD reactants," *Energy Procedia*, vol. 8, pp. 681–687, 2011.

[40] J. A. Aguiar *et al.*, "Atomic scale understanding of poly-Si/SiO_2/c-Si passivated contacts: Passivation degradation due to metallization," in *Proc. IEEE 44th Photovolt. Spec. Conf. PVSC*, 2017, pp. 1–4.

[41] L. Tutsch *et al.*, "Improved passivation of n-type poly-Si based passivating contacts by the application of hydrogen-rich transparent conductive oxides," *IEEE J. Photovolt.*, vol. 10, no. 4, pp. 986–991, Jul. 2020.

[42] B. Nemeth *et al.*, "Effect of the SiO_2 interlayer properties with solid-source hydrogenation on passivated contact performance and surface passivation," *Energy Procedia*, vol. 124, pp. 295–301, 2017.

[43] B. Macco *et al.*, "Atomic-layer-deposited Al-doped zinc oxide as a passivating conductive contacting layer for n^+-doped surfaces in silicon solar cells," *Sol. Energy Mater. Sol. Cells*, vol. 233, Dec. 2021, Art. no. 111386.

[44] L. Tutsch *et al.*, "Improved passivation of n-type poly-Si based passivating contacts by the application of hydrogen-rich transparent conductive oxides," *IEEE J. Photovolt.*, vol. 10, no. 4, pp. 986–991, Jul. 2020.

[45] G. Yang, A. Ingenito, O. Isabella, and M. Zeman, "IBC c-Si solar cells based on ion-implanted poly-silicon passivating contacts," *Sol. Energy Mater. Sol. Cells*, vol. 158, pp. 84–90, 2016.

[46] G. Dingemans, R. Seguin, P. Engelhart, M. C. M. van de Sanden, and W. M. M. Kessels, "Silicon surface passivation by ultrathin Al_2O_3 films synthesized by thermal and plasma atomic layer deposition," *Phys. Status Solidi - Rapid Res. Lett.*, vol. 4, no. 1/2, pp. 10–12, 2010.

[47] R. A. Sinton and A. Cuevas, "Contactless determination of current-voltage characteristics and minority-carrier lifetimes in semiconductors from quasi-steady-state photoconductance data," *Appl. Phys. Lett.*, vol. 69, no. 17, pp. 2510–2512, 1996.

[48] M. Müller, "Reporting effective lifetimes at solar cell relevant injection densities," *Energy Procedia*, vol. 92, pp. 138–144, 2016.

[49] N. M. Terlinden, G. Dingemans, and W. M. M. Kessels, "Role of field-effect on c-Si surface passivation by ultrathin (2–20 nm) atomic layer deposition Al_2O_3," *Appl. Phys. Lett.*, vol. 96, pp. 112101-1–112101-3, 2010.

[50] G. Dingemans and W. M. M. Kessels, "Status and prospects of Al_2O_3-based surface passivation schemes for silicon solar cells," *J. Vac. Sci. Technol. A*, vol. 30, 2012, Art. no. 040802.

[51] G. Dingemans, F. Einsele, W. Beyer, M. C. M. van de Sanden, and W. M. M. Kessels, "Influence of annealing and Al_2O_3 properties on the hydrogen-induced passivation of the Si/SiO_2 interface," *J. Appl. Phys.*, vol. 111, 2012, Art. no. 093713.

[52] P. Padhamnath *et al.*, "Development of thin polysilicon layers for application in monoPoly^{TM} cells with screen-printed and fired metallization," *Sol. Energy Mater. Sol. Cells*, vol. 207, Apr. 2020, Art. no. 110358.

[53] A. Richter *et al.*, "n-type Si solar cells with passivating electron contact: Identifying sources for efficiency limitations by wafer thickness and resistivity variation," *Sol. Energy Mater. Sol. Cells*, vol. 173, pp. 96–105, Mar. 2017.

[54] H. Park *et al.*, "Passivation quality control in poly-Si/SiO_x/c-Si passivated contact solar cells with 734 mV implied open circuit voltage," *Sol. Energy Mater. Sol. Cells*, vol. 189, pp. 21–26, Jan. 2019.

[55] P. Padhamnath *et al.*, "Optoelectrical properties of high-performance low-pressure chemical vapor deposited phosphorus-doped polysilicon layers for passivating contact solar cells," *Thin Solid Films*, vol. 699, Feb. 2020, Art. no. 137886.

[56] G. Dingemans and W. M. M. Kessels, "Status and prospects of Al_2O_3-based surface passivation schemes for silicon solar cells," *J. Vac. Sci. Technol. A Vac., Surf., Films*, vol. 30, no. 4, 2012, Art. no. 040802.

[57] G. T. Yu and S. K. Yen, "Hydrogen ion diffusion coefficient of silicon nitride thin films," *Appl. Surf. Sci.*, vol. 202, no. 1, pp. 68–72, 2002.

[58] G. Dingemans, W. Beyer, M. C. M. van de Sanden, and W. M. M. Kessels, "Hydrogen induced passivation of Si interfaces by Al_2O_3 films and SiO_2/Al_2O_3 stacks," *Appl. Phys. Lett.*, vol. 97, no. 15, 2010, Art. no. 152106.

[59] W. G. J. H. M. Van Sark and F. R. L. Korte, *Physics and Technology of Amorphous-Crystalline Heterostructures Silicon Solar Cells.* Berlin, Germany: Springer, 2012.

[60] G. Dingemans *et al.*, "Stability of Al_2O_3 and Al_2O_3/a-SiN_x:H stacks for surface passivation of crystalline silicon," *J. Appl. Phys.*, vol. 106, 2009, Art. no. 114907.

[61] S. De Wolf and M. Kondo, "Nature of doped a-Si:H/c-Si interface recombination," *J. Appl. Phys.*, vol. 105, no. 10, pp. 103707-1–103707-6, 2009.

[62] T. N. Truong *et al.*, "Hydrogenation mechanisms of poly-Si/SiO_x passivating contacts by different capping layers," *Sol. RRL*, vol. 4, no. 3, pp. 1–6, 2020.

[63] B. W. H. van de Loo, B. Macco, J. Melskens, W. Beyer, and W. M. M. Kessels, "Silicon surface passivation by transparent conductive zinc oxide," *J. Appl. Phys.*, vol. 125, no. 10, pp. 105305-1–105305-1, 2019.

[64] H. E. Çiftpinar *et al.*, "Study of screen printed metallization for polysilicon based passivating contacts," *Energy Procedia*, vol. 124, pp. 851–861, 2017.

[65] D. Chen *et al.*, "24.58% total area efficiency of screen-printed, large area industrial silicon solar cells with the tunnel oxide passivated contacts (i-TOPCon) design," *Sol. Energy Mater. Sol. Cells*, vol. 206, Nov. 2019, Art. no. 110258.